كلية الهندسة بشبرا
FACULTY OF ENGINEERING AT SHOUBRA
ERJ
PRINT ISSN 3009-6049
ONLINE ISSN 3009-6022

ENGINEERING RESEARCH JOURNAL (ERJ)
Volume (53),Issue (3)
July 2024, pp:224-239
https://erjsh.journals.ekb.eg

Impact of Vertical Irregularities on Seismic Response Modification Coefficients of Dual Concrete Shear Wall-Frame Systems

Mina Mounir Naguib [1,*] , tarek abdelgalil [1], mossad ali [1], Mohamed Hamdy Aly [1]

[1] Civil Engineering Department, Faculty of Engineering at Shoubra, Benha University, Cairo, Egypt.
**Corresponding author*

E-mail address: eng.mina.mounir@outlook.com , tarek.abdelgalil@feng.bu.edu.eg , mosaad.ali@feng.bu.edu.eg , mohamed-hamdy@buc.edu.eg

Abstract: This study investigates the impact of vertical irregularities on the seismic response modification coefficients (R factors) of dual concrete shear wall-frame systems. Three-dimensional models of 5-, 10-, and 15-story buildings were developed, adhering to the design provisions of the Egyptian Code for the Design of Concrete (ECP 203, 2020) and considering loads specified by the Egyptian Code for Loads (ECP 201, 2012). Two types of vertical irregularities - geometrical and in-plane discontinuity - were introduced at three distinct locations (base, one-third, and two-thirds of the height) with varying severity levels. Pushover analysis was employed to evaluate the seismic behavior of the structures and determine their response. The primary objective was to assess the influence of these irregularities on R factors and compare them with code recommendations. The results indicate that the R factor exhibits an inverse proportionality with respect to the presence of dual systems. Geometric irregularities decrease R factors in structures with 5 or fewer stories, followed by a peak in 10-story structures and a gradual decrease for taller buildings. Conversely, geometric irregularities appear to have an inverse effect on the influence of in-plane discontinuities on R factors. Structures with 5 or fewer stories experience an increase in R factors with increasing discontinuity, peaking in 10-story structures, and then decreasing with height. The average R factor across all configurations was 5.8, with a maximum value of 9.78 observed in 5-story structures with specific discontinuity irregularities. This investigation provides valuable insights into the seismic performance of dual concrete systems subjected to vertical irregularities. The findings highlight the importance of considering these irregularities when determining R factors for seismic design, potentially leading to more accurate and performance-based design approaches.

Keywords: Seismic response, Pushover analysis, In-plane discontinuity, Vertical geometric irregularity.

1. Introduction

Structural irregularities in buildings are commonly attributed to architectural demands, modifications during the design phase, and alterations in the building's purpose over its operational life. Contemporary seismic design codes distinguish between plan and vertical irregularities. Plan (horizontal) irregularities arise from factors such as discontinuities in the lateral force resisting system (LFRS) outside its plane (out-of-plane offset). Vertical irregularities may result from notable variations in stiffness, strength, mass, dimensions, or discontinuities within the LFRS plane. This distinction between plan and elevation irregularities is also evident in the literature. While there is a growing interest in examining the seismic behavior of building irregularities, particularly vertical ones, the literature lacks a systematic coverage of the impacts of various types of vertical irregularities on the seismic design of buildings.

For steel structure. In a study by Humar and Wright [3], the dynamic behavior of multistorey steel rigid-frame buildings with set-back towers is investigated, the findings highlight that higher modes of vibration in set-back buildings significantly contribute to seismic response, especially with slender towers. For concrete structure, Aranda [4] made a comparison of ductility demands between set-back and regular structures by using ground motions recorded on soft soil and observed higher ductility demands for set-back structures than for the regular ones and found this increase to be more pronounced in the tower portions. Shahrooz and Moehle [5] investigated the impact of setback irregularity on earthquake response in multi-story buildings, damage concentration in tower members was observed due to high torsional ductility, indicated that the fundamental mode predominantly influenced the response parallel to the setback irregularity. Wood [6] studied the seismic response of reinforced concrete frames with setback irregularities using two small-scale model structures—one with symmetric setbacks and the other with unsymmetric setbacks, concluded that there is not much difference in the seismic response between regular and setback structures. Ruiz et al. [7] investigated the seismic performance of structures with a weak first story (WFS) under a single ground motion. They focused on the impact of lateral strength discontinuity on ductility demand at the first story, the study included parametric analyses for five and twelve-story structures with WFS, concluded that the response of WFS buildings depends on factors such as the ratio of dominant periods of seismic force and response, the resistances of upper and first stories, and the seismic coefficient used for design. Mwafy and Khalifa [8] conducted a study on vertical irregular structures, focusing on common types of irregular high-rise

buildings in the United Arab Emirates, a medium seismicity region. They selected five 50-story reinforced concrete buildings representing various irregularities, including extreme soft story, geometric, in-plane discontinuity, and extreme weak story irregularities. The study concluded that different types of irregularities impact seismic design response factors differently. Lateral force resisting system discontinuity and soft story irregularity have the most significant effects on seismic factors and local seismic response. The results suggest that response factors for regular and moderately irregular structures can increase by around ten percent, while the Cd factor decreases by the same ratio. According to ASCE 7, the R factors for models with medium or no irregularity can be increased to 4.5, with a corresponding decrease in the Cd factor to 3.5. However, due to the substantial impact of irregularities on local and global structural response, the conservative R and Cd factors recommended by the design code should be maintained for structures with discontinuity in the lateral force resistance system and soft story irregularity.

An analytical model of a structure that accounts for all sources of stiffness, P-delta effects, and therefore the inelastic response is the most accurate approach for seismic design. The code-specified factor is known as the response modification factor, which represents the ratio between the required base shear forces to keep the structure elastic during the earthquake and the design base shear force considering its inelastic behavior.

The Egyptian code for loads [2] classified the R-factor according to the construction material, the structural system, and the ductility level. A dual system, which is stated in the code as a system combined of moment-resisting space frames and shear walls, is classified as having: a) sufficient ductility; b) limited ductility. Moreover, the R-factor is given discrete values for each system depending on the stated classifications. However, these discrete values are assigned to structural systems in an unclear way, and their use can be very simple in the design process [1]. This simplicity may lead to an approximate design. That is why this research study mainly focuses on evaluating the response modification factor and its components for reinforced concrete dual systems at their ultimate capacity stage, near failure. The criteria used for the evaluation of the R-factor through its components is the nonlinear static pushover analysis using both material and geometrical nonlinearity of the static dual systems, which are modeled according to the limitations [1]. Moreover, these systems are loaded according to the standards of the Egyptian code for loads [2], and then they are designed according to the provisions of the Egyptian code for design of RC structures [1]. After the processes of modeling, loading, and analyzing, the pushover curve can be plotted for each dual system model to obtain the R-factor at failure.

The main aim of this study is to estimate the R-factor for various irregularly reinforced concrete dual systems at failure according to the Egyptian Code for Calculation of Loads and Forces for Buildings (ECP-201), 2012 [2], using pushover analysis and finite element software programs. Investigation is made for the effect of stiffness modifiers for columns, beams, and shear walls on the response modification factor for reinforced concrete dual systems. Comparison of the values of several parameters, such as base shear, top displacement, story displacement, inter-story drift, ductility reduction factor and overstrength factor are made.

2. METHODOLOGY

To get the response modification factor through different types of concrete structure systems suffering from different types of vertical irregularities, a study plan consisting of 42 models has been proposed to probe the dual system response under the effect of different irregularities. All models were designed according to ECP 203, 2020[1], and all loads applied, whether static or seismic, according to ECP 201, 2012[2], by using the incremental pushover analysis and the values of the response modification factor at failure following the Egyptian code needs. The proposed analysis includes dual systems, style methodology, nonlinear analysis procedures, and performance analysis conducted by a mathematical model using the software package SAP2000 version 18.2 [9].

Various configurations of reinforced concrete statical systems designed for residential buildings are examined, focusing primarily on wall-frame systems. The suggested statical system encompasses structures with varying numbers of stories: 5, 10, and 15, each with a standard story height of 3.0 m. These systems exhibit irregularities in both plan and elevation. The mathematical models presented in the thesis are categorized into two types: wall-frames with the influence of vertical geometric irregularity, and wall-frames with the influence of in-plane discontinuity.

Specify the load cases, target displacement, its position, and load combinations. Execute the analysis, present the static pushover curve (illustrating base shear against top displacement), and utilize these outcomes in computing the "R" components. Calculating the R value enables a comparison of results against the prescribed values in ECP201- 2012 [2], and UBC1997 [10] standards, facilitating recommendations and leading to the observation whether the codes are conservative.

3. FINITE ELEMENT MODEL

The characteristics of the analyzed frame-wall systems, the methodology for their design, nonlinear analysis procedures, and performance evaluations are carried out through a mathematical model using computer-integrated software. SAP2000 version 18.2 [9] is the software package employed for this study. All systems adhere to the regulations outlined in ECP 203[1], and the application of loads follows the guidelines of ECP 201[2], as detailed in Table (1).

3.1 Material Specifications

The structural model incorporates distinct material properties for columns, slabs, and beams as shown in Table 2. For columns, a confined concrete model is used. This multilinear representation is characterized by specific

properties Fig.1-a. Conversely, slabs and beams are modeled with unconfined concrete, sharing similar properties with the confined type Fig.1-b. In addition to concrete materials, reinforcing steel is characterized by bilinear properties, ensuring a realistic representation of the structural components for accurate analysis under various loading conditions Fig.1-c.

3.2 Frame Element

Frame objects, used to model columns, and beams in 3D system model, the geometry is straight lines which connect with two nodes at it's at the start and end of frame element. Torsion, biaxial bending, biaxial shear, and axial deformation are all taken into consideration for in the beam and column formulation.

3.3 Shell Element

A shell is a four-node area object used to model slabs. The nonlinearity of vertical element only taken into consideration so as it significantly affects the shape of the total displacement of the model during the impact of earthquake forces.

3.4 Multi-Layer Shell Element

The multi-layer shell element is according to the principles of composite material mechanics. It is consisting of a number of layers with different thicknesses and different material properties, like concrete layers or reinforcement layers. The strains and curvatures of the middle-layer of the shell element are firstly obtained during the calculation, and the strains in other layers can be determined based on the assumption. Then, the stress in each layer can be calculated through the material constitutive law, and the internal force of the shear element (force and bending moment along the section) can be determined through the numerical integration of the stress in all layers. The advantage of multi-layer shell element is its capability of simulating coupled in-plane or out-of-plane bending as well as in-plane direct shear and coupled bending-shear behavior of reinforced concrete shear walls. The reinforcement rebars are simulated into one or more layers and these rebar layers can be isotropic or orthotropic depending on the reinforcement ratio in the longitudinal and transverse directions.

3.5 Plastic Hinge Modelling

Plastic hinges are assigned in different degrees of freedom, one degree of freedom for beam cross-section the plastic hinges assigned as (M2-M3), and two degrees of freedom assigned for column element as (P-M2-M3). The position where the hinges assigned to the element is at 0.1 and 0.9 of its total length where the high stress and elastic deformation occurs.

TABLE 1. The applied loads and load combinations

Gravity Loads	-floor covering = 1.47 kN/m^2. -Walls load = 3.43 kN/m^2. -Live load (residential category) = 1.96 kN/m^2.
Seismic Loads	$F_b=S_d(T_1)\,\lambda\frac{W}{g}$
Load combination	U = 1.40 D + 1.60 L U = 1.12 D + α L ± S

TABLE 2. The adopted material properties

Material properties for columns, beams, and the concentrated reinforcement regions of the shear walls	Unit weight γc = 25 kN/m³ characteristic strength fcu = 2.451 kN/cm^2 modulus of elasticity Ec = 140000√fcu Poisson's ratio μc = 0.20
Material properties for slabs and the distributed reinforcement regions of the shear walls	Unit weight γc = 25 kN/m³ characteristic strength fcu = 2.451 kN/cm^2 modulus of elasticity Ec = 140000√fcu Poisson's ratio μc = 0.20
Material properties of steel that will be used as the reinforcement of the columns, the beams, and the shear walls.	Unit weight γs = 78.49 kN/m³ Yield strength fy = 35.30 kN/cm^2 Ultimate Yield strength fyu = 50.99 kN/cm^2 modulus of elasticity Es = 196.1X10^6 kN/m^2 Poisson's ratio μs = 0.30

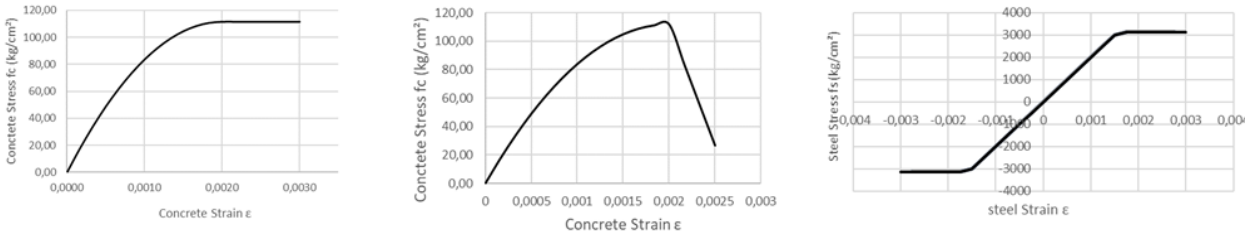

FIGURE 1. Stress-strain curve adopted for the different materia

4. NONLINEAR PUSHOVER ANAYSIS STEPS AND 'R' FACTOR CALCULATION

The following steps are used to create the nonlinear pushover analysis for all models:

1- Draw the model for each case then define section properties for column, beam, slab, and walls then assign for the model.

2- Construct the load patterns then assign them to the model.

3- Define the load cases sequentially as nonlinear static cases; dead load case as zero initial condition (starts from unstressed state), super imposed (combines floor cover and wall load patterns) and continues from the end of the dead load case, live load case continues from the end of superimposed load case, and finally the pushover load case (that contains the static lateral loads pattern) and continues from the end of live load case.

4- Define the targeted monitored displacement and its position at the top of each model with multi states so that the deformed shape can be seen.

5- Define the load combination (Ultimate load combination-earthquake load combination and working combination so that to be used at hinges definition.

6- Define the frame hinges for beams and columns, with the option of no hinges overwrites to show both of beam and column in each joint.

7- Run the analysis then when it finishes, display the static pushover curve (base shear versus top displacement) to use it in the calculations of "R" components.

8- Calculate ductility reduction factor R_μ by the following equation by Miranda and Bertero [11].

$$R_\mu = (\mu - 1)\frac{T}{Tc} + 1 \qquad T < Tc \qquad (1)$$

$$R_\mu = \mu \qquad T \geq Tc \qquad (2)$$

where T is the fundamental period of the structure taken from SAP model, and Tc is the characteristic period at the end of acceleration which equal to 0.25 s.

9- Calculate overstrength factor R_s by the following equation according to ASCE 7-16 [12]

$$R_s = \frac{Vy}{Vd} \qquad (3)$$

Where: V_y yield force (maximum base force taken from SAP [9]), V_d the design force (deduced from ECP 201[2]).

10- Then multiply both ductility reduction factor and overstrength factor to get actual response factor

$$R = R_\mu \times R_s \qquad (4)$$

5. VERIFICATION OF PUSHOVER ANALYSIS METHOD

5.1 Model 1

Cansız [13] conducted a study on reducing weak-soft-story irregularities in RC structures during earthquakes using Seism-Build software [14]. Sixty structures were analyzed focusing on cross-frames' efficacy in buildings with RC walls and weak-story issues. The building information is detailed in Table 3. Validation has been conducted using SAP2000 [9] for the G+2 irregular ground soft story model by increasing the height of the ground story. Fig. 3 illustrates the difference between the two pushover curves obtained from [13] and the current study, showing remarkably similar results. Fig. 2 illustrate the 3D model studied to verify pushover analysis.

TABLE 1. Building properties for modeling G+2 of Cansız [13].

Plan size	15 × 15 m'
Building height	10 m'
Type of structure	Multi story RC frame (G+2)
Story height	Ground floor 4m, remaining floors 3m.
Bay width	5 m, Bays in x and y directions
Bay number	3 at each direction
Beam	300mm×500mm.
Column [corner and inner, edge]	400mm×400mm, 350mmx500mm
Slab	140mm
Support Conditions	Fixed
Importance Factor	I = 1
Response Reduction Factor	R = 5
Concrete, Density	fcu= 30 MPa, 30 kN/m^3
Steel	fy= 415 MPa
Imposed load	1.992 kN/m^2
Floor finishes load	1.494 kN/m^2
Wall load on beam	3.487 kN/m^2
Equivalent lateral loads	ASCE-41-17

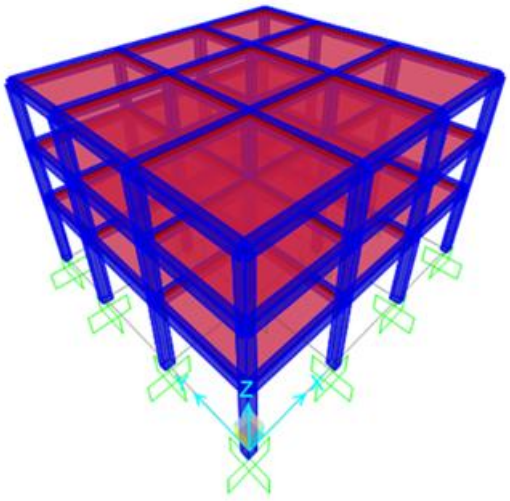

FIGURE 2. 3D view of model 1.

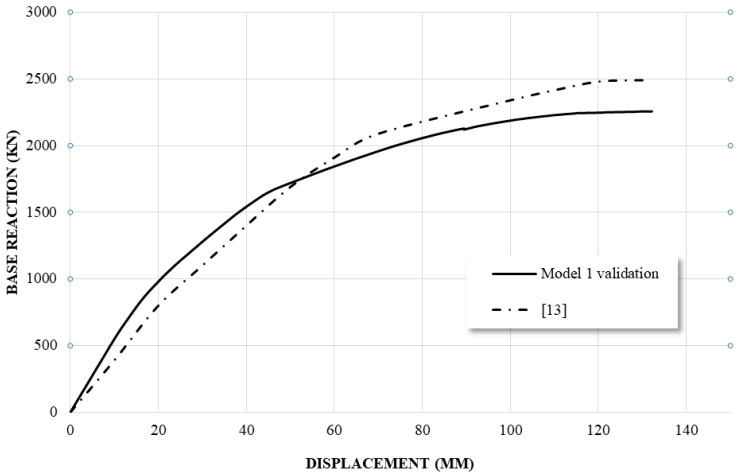

FIGURE 3. Displacement-base shear curve obtained by [13] and current validation study.

5.2 Model 2

An additional validation was carried out on a six-story concrete frame, conducted by Vandit [15]. The finite element method utilized for modeling reinforced concrete ductile frames was SAP2000 [9]. The frames were designed in accordance with the provisions outlined in the Indian Standard Design Code [16]. Details regarding the building are listed in Table 4, also Fig. 4 indicating 3D-model studied for verification.

TABLE 4. Building properties for modeling Vandit [15].

Number of stories	G + 5
Floor Height	3 m
Materials	Concrete (M25); Steel Reinforcement (Fe415)
Size of Beams	230 x 450 mm
Size of Column	500 x 500 mm
Depth of slab	150 mm
Specific weight of infill	20 kN/m^3
Specific weight of RCC	25 kN/m^3
Type of soil	Medium Soil
Impose load	3 kN/m^2
Importance factor	1.2
Seismic zone	v
Zone Factor	0.36

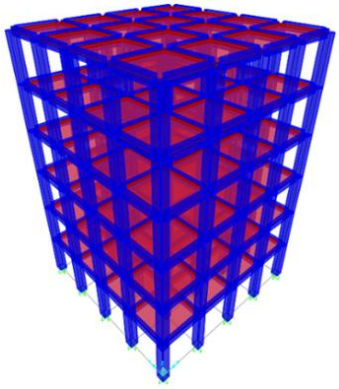

FIGURE 4. 3D view of model 2.

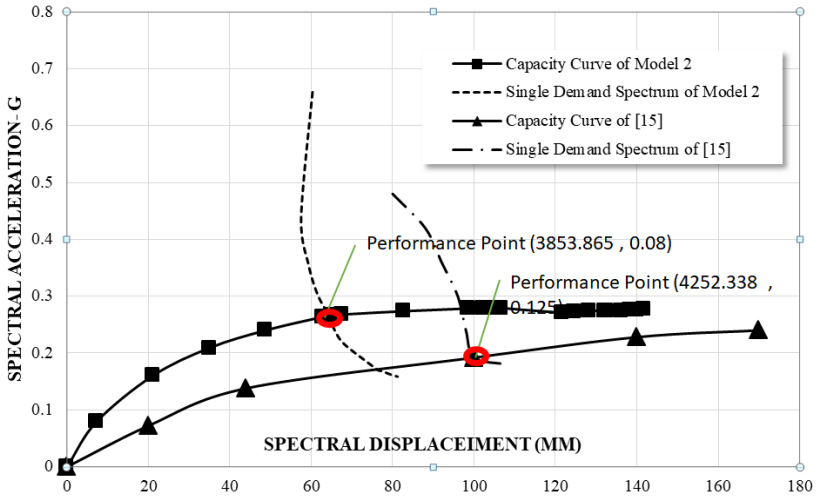

FIGURE 5. Comparison of results of ATC40 curve of [15] and current validation.

As shown in Fig. 5, the difference of two performance point from 4252 obtained by Vandit [15], and 3853 through current validation, is only 9.0% which is acceptable variance because [15] did not consider the details of reinforcement of the model so there is a difference in results.

5.3 Model 3

A further validation was conducted using the findings from a 5-story L-shaped RC model by Tarsha and Fattoum [17]. The study showcased results from analyzing 17 models through nonlinear static analysis using SAP2000. The structural system of the model comprises a frame-wall system with 5, 10, and 15 stories, incorporating re-entrant corner irregularities. Frame participation in resisting shear force ranges from 25% to 60%. General building information is provided in Table 5, and the displacement-base shear curve depicted in Fig. 7 was found to be identical. Also Fig. 6 indicating 3D-model studied for verification.

TABLE 5. Building properties of modeling L-Shape Five-story case studied by [17]

Thickness of slab used	12 cm
Dim of Beams	25x45 cm
Dim of column	30x50 cm
Hight of story	3.5 m’
Each bay for X and Y direction	5 m’
Soil type	Sd
Ca	0.44
Cv	0.64
Na	1
Nv	1
R	6
Mass	DL +0.25LL
code	UBC 97

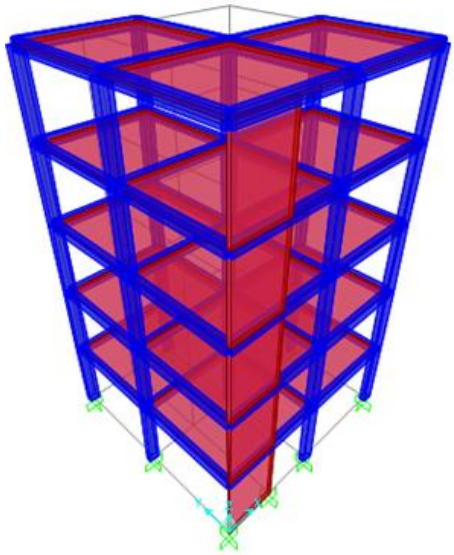

FIGURE 6. 3D view of model 3.

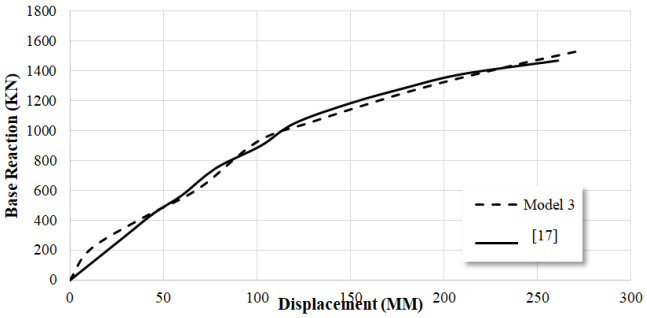

FIGURE 7. Comparison between displacement-base shear curve of L shape model obtained by [17] and current validation.

6. NUMERICAL STUDY OF THE EFFECT OF GEOMETRICAL IRREGULARITY.

6.1 Description of models and studied parameters

Validation with previous research and studies confirms the efficacy of the proposed model in accurately simulating the structural behavior of buildings. The proposed systems across all models comprise varying numbers of stories, including configurations of 5, 10, and 15 stories, each with a standard story height of 3.0 m. The typical bay length is 5.0 m, with three typical bays in each direction for every model. In concrete sections, as illustrated in Fig. 8 and detailed in Tables 6 and 7, all columns are assumed to be square. Concrete cover is set at 25 mm, stirrups are 8 mm in diameter, and longitudinal bars, listed in Tables 6 and 7, adhere to the limits specified in ECP 203 [1]. Rectangular section shear walls have L/b ratio equal to 6.67 (greater than 5.0) with a concentrated reinforcement ratio equals to 3.0% in edge length of the wall and distributed reinforcement ratio equals to 0.40% in middle length of the wall. The columns and walls are considered fixed to the foundation. Concrete slabs are designed considering the combination of gravity loads per ECP 201 [2] and ECP 203 [1]. Longitudinal and transverse bars at M' have a diameter of 5 Φ10 mm, with a 140 mm thickness and a concrete cover of 20 mm, as depicted in Fig. 8.

In the study of irregularities, each set of floors includes a control structure with uniform stiffness across all floors. Additionally, three structures with geometrical irregularity are examined. The first structure has geometric irregularity applied to 1^{st}, 2^{nd} and 3^{rd} level of H5, H10 and H15 sequentially. For the second group, geometric irregularity applied to 2^{nd}, 4^{th} and 5^{th} level of H5, H10 and H15 sequentially. The third position the geometric irregularity located at 3^{rd}, 7^{th} and 10^{th} level of H5, H10 and H15 sequentially for the third group. It is essential to note that each structure with a geometrical irregularity is investigated under different values, specifically 1.2, 1.3, and 1.4 relative to the control structure. The geometrical irregularity characteristics vary by adjusting the width of the shear wall, introducing a comprehensive exploration of the impact of geometrical irregularity on structural behavior. Table 8 and fig. 9 summarize the studied structures with different irregularities conditions.

TABLE 6. Beams concrete dimension in mm and RFT.

Model	H5				H10				H15			
Beam number	B1	B2	B3	B4	B1	B2	B3	B4	B1	B2	B3	B4
Ground	300X900 5Φ25	300X900 4Φ25	300X900 5Φ25	300X900 4Φ25	300X700 5Φ22	250X700 4Φ22	300X700 5Φ22	300X700 5Φ18	300X700 5Φ22	250X700 4Φ22	300X700 5Φ22	250X700 4Φ22
First	300X900 5Φ25	300X900 4Φ25	300X900 5Φ25	300X900 4Φ25	300X700 5Φ22	250X700 4Φ22	300X700 5Φ22	300X700 5Φ18	300X700 5Φ22	250X700 4Φ22	300X700 5Φ22	250X700 4Φ22
Second	300X900 4Φ25	300X800 5Φ22	300X900 4Φ25	300X800 4Φ25	300X700 5Φ22	250X700 4Φ22	300X700 5Φ22	300X700 5Φ18	300X700 5Φ22	250X700 4Φ22	300X700 5Φ22	250X700 4Φ22
Third	300X800 6Φ18	300X800 5Φ18	300X800 6Φ18	300X800 6Φ18	300X700 5Φ22	250X700 4Φ22	300X700 5Φ22	300X700 5Φ18	300X700 5Φ22	250X700 4Φ22	300X700 5Φ22	250X700 4Φ22
Fourth	300X700 4Φ16	250X700 4Φ16	300X700 4Φ16	300X700 4Φ16	250X700 4Φ22	250X700 5Φ18	250X700 4Φ22	250X700 4Φ18	300X700 5Φ22	250X700 4Φ22	300X700 5Φ22	250X700 4Φ22
Fifth	———	———	———	———	250X700 4Φ22	250X700 5Φ18	250X700 4Φ22	250X700 4Φ18	250X700 4Φ22	250X700 4Φ22	300X700 5Φ22	250X700 4Φ22
Sixth	———	———	———	———	250X700 4Φ18	250X700 4Φ18	250X700 4Φ22	250X700 4Φ18	250X700 4Φ22	250X700 5Φ18	250X700 4Φ22	250X700 5Φ18
Seventh	———	———	———	———	250X700 4Φ16	250X700 4Φ16	250X550 5Φ18	250X550 4Φ18	250X700 4Φ22	250X700 5Φ18	250X700 4Φ22	250X700 5Φ18
Eighth	———	———	———	———	250X550 4Φ18	250X550 3Φ16	250X550 5Φ18	250X550 4Φ18	250X700 5Φ18	250X700 5Φ18	250X700 4Φ22	250X700 5Φ18
Ninth	———	———	———	———	250X550 4Φ12	250X550 3Φ16	250X550 4Φ12	250X550 4Φ12	250X700 5Φ18	250X700 4Φ18	250X700 5Φ18	250X700 5Φ18
Tenth	———	———	———	———	———	———	———	———	250X700 5Φ18	250X700 4Φ18	250X700 5Φ18	250X700 4Φ18
Eleventh	———	———	———	———	———	———	———	———	250X700 4Φ18	250X550 4Φ18	250X700 5Φ18	250X700 4Φ18
Twelfth	———	———	———	———	———	———	———	———	250X700 4Φ18	250X550 4Φ18	250X700 4Φ18	250X550 4Φ18
Thirteenth	———	———	———	———	———	———	———	———	250X550 4Φ18	250X550 3Φ16	250X700 4Φ18	250X550 4Φ18
Fourteenth	———	———	———	———	———	———	———	———	250X550 3Φ16	250X550 3Φ16	250X700 4Φ18	250X550 3Φ16

TABLE7 . Columns concrete dimension in mm and RFT.

Model	H5			H10			H15		
Column number	C1	C2	C3	C1	C2	C3	C1	C2	C3
Ground	350-6Φ18	400-8Φ16	450-6Φ22	450-8Φ18	550-12Φ18	650-12Φ22	550-8Φ22	600-8Φ25	750-12Φ25
First	300-6Φ16	350-8Φ16	400-6Φ22	450-8Φ18	550-12Φ18	650-12Φ22	550-8Φ22	600-8Φ25	750-12Φ25
Second	250-4Φ16	300-6Φ16	350-6Φ18	400-8Φ16	550-12Φ18	550-8Φ22	500-8Φ22	550-8Φ22	700-10Φ25
Third	250-4Φ12	250-6Φ12	300-4Φ18	400-8Φ16	450-12Φ16	550-8Φ22	500-8Φ22	550-8Φ22	700-10Φ25
Fourth	250-4Φ12	250-4Φ12	250-4Φ16	350-8Φ16	450-12Φ16	500-8Φ22	450-8Φ18	500-8Φ22	600-8Φ25

Fifth	———	———	———	350-8Φ16	450-12Φ16	500-8Φ22	450-8Φ18	500-8Φ22	600-8Φ25
Sixth	———	———	———	300-8Φ12	350-8Φ16	450-8Φ18	400-8Φ18	450-8Φ18	550-8Φ25
Seventh	———	———	———	300-8Φ12	350-8Φ16	450-8Φ18	400-8Φ18	450-8Φ18	550-8Φ25
Eighth	———	———	———	250-4Φ12	350-8Φ16	350-8Φ16	350-8Φ16	400-8Φ18	500-8Φ22
Ninth	———	———	———	250-4Φ12	250-4Φ16	350-8Φ16	350-8Φ16	400-8Φ18	500-8Φ22
Tenth	———	———	———	———	———	———	300-8Φ12	350-8Φ16	400-8Φ18
Eleventh	———	———	———	———	———	———	300-8Φ12	350-8Φ16	400-8Φ18
Twelfth	———	———	———	———	———	———	250-4Φ16	300-8Φ12	350-8Φ16
Thirteenth	———	———	———	———	———	———	250-4Φ16	300-8Φ12	350-8Φ16
Fourteenth	———	———	———	———	———	———	250-4Φ12	250-4Φ12	250-4Φ16

TABLE 8. Configurations of the First system.

Specimen name	Number of stories	Type of irregularity	Severity of irregularity	Place of influence	Group
WB1-H5	5	------	------	------	WB1-H5
WB1-H5-1.2L-D	5	Geometric	Li >1.2L1	First floor	
WB1-H5-1.3L-D	5	Geometric	Li >1.3L1	First floor	
WB1-H5-1.4L-D	5	Geometric	Li >1.4L1	First floor	
WB1-H5-1.2L-O	5	Geometric	Li >1.2L1	Second floor	
WB1-H5-1.3L-O	5	Geometric	Li >1.3L1	Second floor	
WB1-H5-1.4L-O	5	Geometric	Li >1.4L1	Second floor	
WB1-H5-1.2L-T	5	Geometric	Li >1.2L1	Third floor	
WB1-H5-1.3L-T	5	Geometric	Li >1.3L1	Third floor	
WB1-H5-1.4L-T	5	Geometric	Li >1.4L1	Third floor	
WB1-H10	10	____	____	____	WB1-H10
WB1-H10-1.2L-D	10	Geometric	Li >1.2L1	Second floor	
WB1-H10-1.3L-D	10	Geometric	Li >1.3L1	Second floor	
WB1-H10-1.4L-D	10	Geometric	Li >1.4L1	Second floor	
WB1-H10-1.2L-O	10	Geometric	Li >1.2L1	Fourth floor	
WB1-H10-1.3L-O	10	Geometric	Li >1.3L1	Fourth floor	
WB1-H10-1.4L-O	10	Geometric	Li >1.4L1	Fourth floor	
WB1-H10-1.2L-T	10	Geometric	Li >1.2L1	Seventh floor	
WB1-H10-1.3L-T	10	Geometric	Li >1.3L1	Seventh floor	
WB1-H10-1.4L-T	10	Geometric	Li >1.4L1	Seventh floor	
WB1-H15	15	____	____	____	WB1-H15
WB1-H15-1.2L-D	15	Geometric	Li >1.2L1	Third floor	
WB1-H15-1.3L-D	15	Geometric	Li >1.3L1	Third floor	
WB1-H15-1.4L-D	15	Geometric	Li >1.4L1	Third floor	
WB1-H15-1.2L-O	15	Geometric	Li >1.2L1	Fifth floor	
WB1-H15-1.3L-O	15	Geometric	Li >1.3L1	Fifth floor	
WB1-H15-1.4L-O	15	Geometric	Li >1.4L1	Fifth floor	
WB1-H15-1.2L-T	15	Geometric	Li >1.2L1	Tenth floor	
WB1-H15-1.3L-T	15	Geometric	Li >1.3L1	Tenth floor	
WB1-H15-1.4L-T	15	Geometric	Li >1.4L1	Tenth floor	

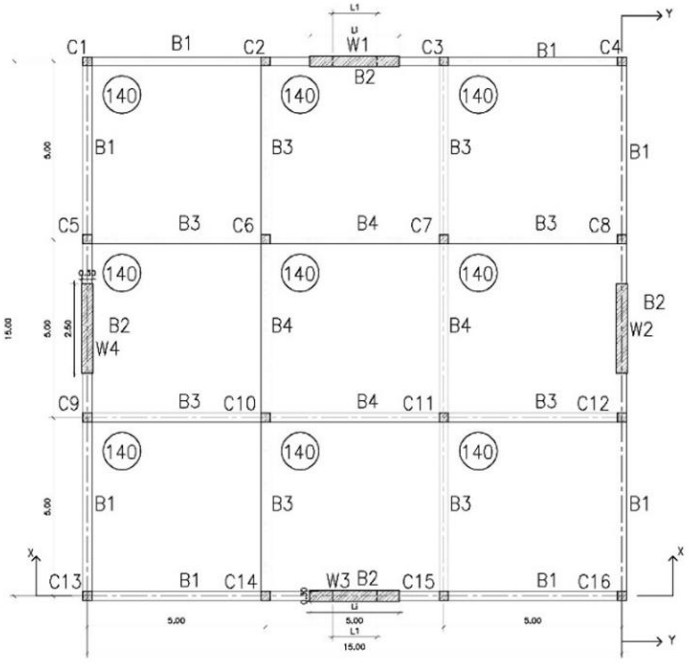

FIGURE 8. The structure plan of WB1

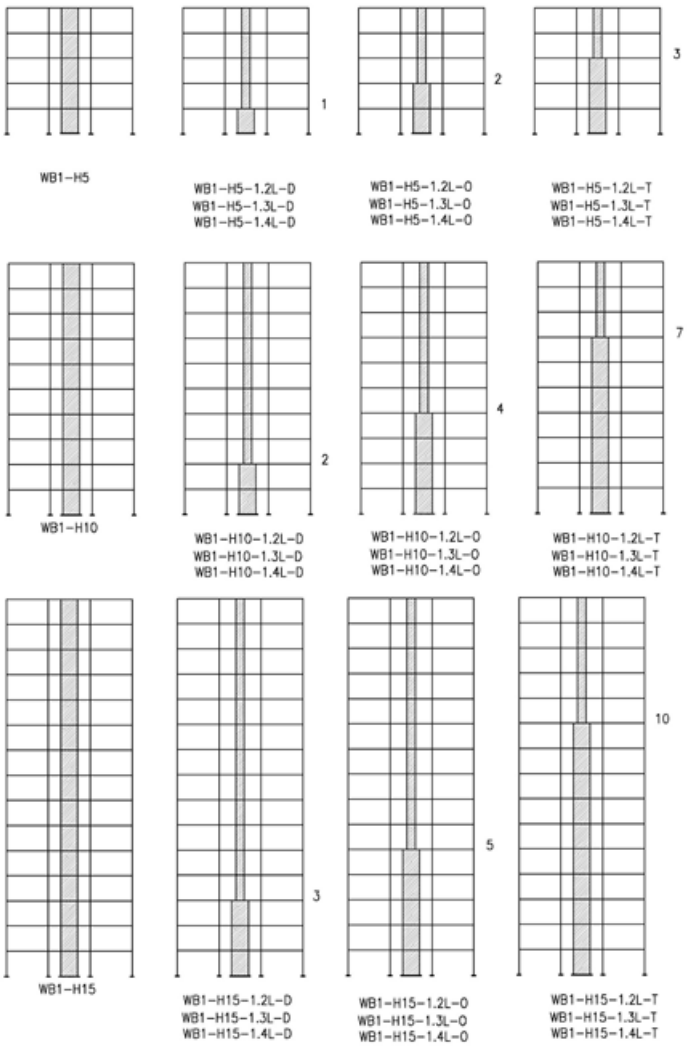

FIGURE 9. Dual system with effect of geometrical irregularity.

6.2 Results and discussion

The SAP 2000 [9] software was utilized to conduct nonlinear static pushover analysis on these systems. Subsequently, equations 1 through 4 were applied sequentially to derive the ductility reduction factor (Rμ), overstrength factor (Rs), and response factor (R). The outcomes of these calculations are presented in Table 9.

TABLE 9. Calculations of "R" components for Third system.

Specimen name	Rμ	Rs	R	R relative Geometry	R relative Geometrical irregularity	Top Displacement (mm)
WB1-H5	2.24	5.59	12.52	0%	0%	49.6
WB1-H5-1.2L-D	1.47	4.86	7.14	-43%	-43%	71.6
WB1-H5-1.3L-D	1.88	4.79	9.01	-28%	-28%	166.2
WB1-H5-1.4L-D	1.59	4.89	7.77	-38%	-38%	43.8
WB1-H5-1.2L-O	1.97	4.72	9.28	-26%	-26%	91
WB1-H5-1.3L-O	2.05	5.85	12.01	-4%	-4%	171.7
WB1-H5-1.4L-O	1.68	5.66	9.53	-24%	-24%	44.1
WB1-H5-1.2L-T	1.9	5.26	10.02	-20%	-20%	84.2
WB1-H5-1.3L-T	1.83	5.58	10.19	-19%	-19%	173.7
WB1-H5-1.4L-T	1.79	4.3	7.71	-38%	-38%	49.2
WB1-H10	1.3	3.81	4.95	-60%	0%	98.7
WB1-H10-1.2L-D	1.55	4.11	6.35	-49%	28%	201
WB1-H10-1.3L-D	1.4	3.94	5.5	-56%	11%	39.8
WB1-H10-1.4L-D	1.48	4.18	6.2	-50%	25%	98.6
WB1-H10-1.2L-O	1.6	4.31	6.91	-45%	40%	164.2
WB1-H10-1.3L-O	1.35	3.84	5.2	-58%	5%	58.7
WB1-H10-1.4L-O	1.31	3.84	5.03	-60%	2%	75.8
WB1-H10-1.2L-T	1.39	4.09	5.69	-55%	15%	170.5
WB1-H10-1.3L-T	1.31	3.84	5.04	-60%	2%	57.9
WB1-H10-1.4L-T	1.59	4.3	6.82	-46%	38%	77.6
WB1-H15	1.62	3.76	6.1	-51%	0%	170.1
WB1-H15-1.2L-D	1.65	3.74	6.16	-51%	1%	46.4
WB1-H15-1.3L-D	1.63	3.72	6.09	-51%	0%	85.2
WB1-H15-1.4L-D	1.8	3.93	7.05	-44%	16%	170.6
WB1-H15-1.2L-O	1.64	3.68	6.04	-52%	-1%	51.3
WB1-H15-1.3L-O	1.56	3.72	5.82	-54%	-5%	73.6
WB1-H15-1.4L-O	1.65	3.69	6.1	-51%	0%	184.1
WB1-H15-1.2L-T	1.64	3.75	6.17	-51%	1%	35.3
WB1-H15-1.3L-T	1.66	3.86	6.42	-49%	5%	98.5
WB1-H15-1.4L-T	1.67	3.76	6.28	-50%	3%	171

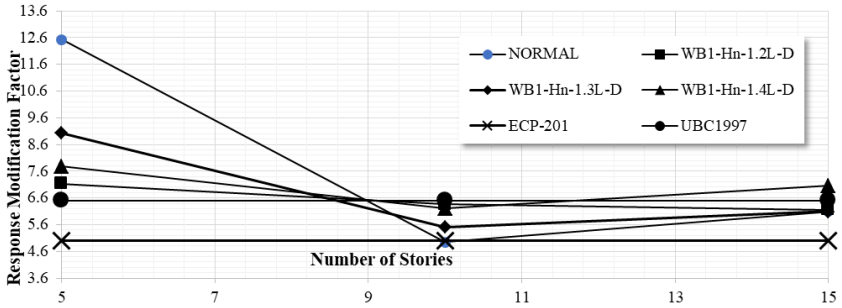

FIGURE 10. Response modification factors versus number of stories for the first system models with geometrical distribution located in the lower part, in normal, regular, irregular, and extreme.

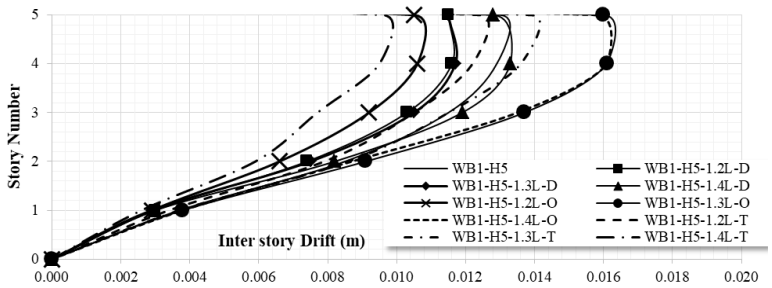

FIGURE 11. Story inter-drift profile for WB1-H5 with regular, irregular and extreme case.

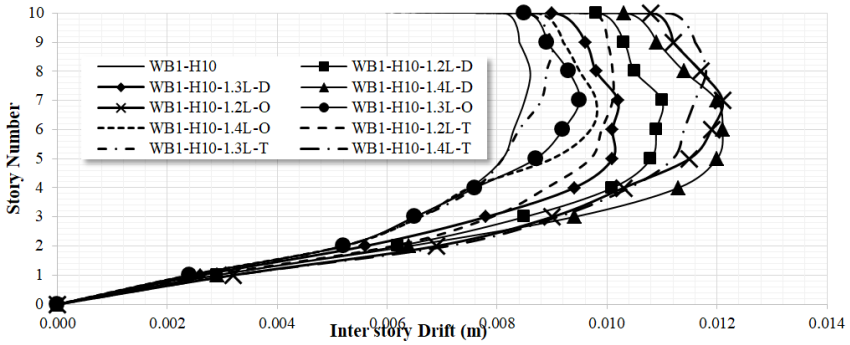

FIGURE 12. Story inter-drift profile for WB1-H10 with regular, irregular and extreme case.

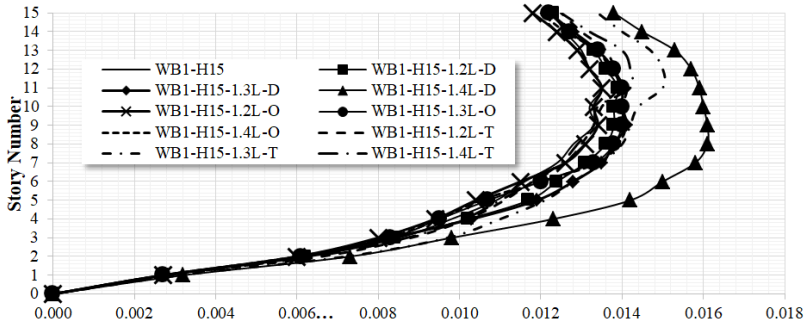

FIGURE 13. Story inter-drift profile for WB1-H15 with regular, irregular and extreme case.

As shown in Table 9 and Fig.10 according to the change in structure high, for WB1-H15 case, the response modification factor is decreased by 51%. Then, increased by 60% for WB1-H10. According to the change in geometrical distribution, for WB1-H5-1.2L-D the R factor decreased by 43%, for WB1-H10-1.2L-O there was a significant increase in R value by 40% and for WB1-H15-1.4L-O there is no change in R factor.

As shown in Table 9, in WB1-H5 model, the story displacement is highly affected by the geometrical irregularity. While WB1-H5-1.2L-D, the displacement of the fifth story decreased by 11.69%, while the first story did not affect it remarkably. In cases WB1-H5-1.4L-T, the displacement of the fifth story decreased by 28.83%, while the first story did not affect it remarkably.

Second, for WB1-H10 model, the story displacement is highly affected by the geometrical irregularity. As shown in Table 9, while WB1-H10-1.4L-D, the displacement of the 10-story increased by 37.85%, while the first story did not affect it remarkably. In case WB1-H10-1.2L-O, the displacement of the 10-story increased by 37.71%. In the case WB1-H10-1.4L-T, the displacement of the 10-story increased by 37.57%.

Third for WB1-H15 model the story displacement is moderately affected with the geometrical irregularity. As shown in Table 9, while WB1-H15-1.4L-D, the displacement of the 10-story increased by 20.94%, while the first story did not affect it remarkably. In the case WB1-H15-1.3L-O, the displacement of the 10-story increased by 2.59%. In the case WB1-H15-1.3L-T, the displacement of the 10-story increased by 10.77%, while in the case of an irregularity of 1.4, the displacement increased by 2.89%.

As shown in Fig.11, for WB1-H5 model, the inter-story drift of 5-story didn't change in WB1-H5-1.4L-D case, while at WB1-H5-1.2L-D and WB1-H5-1.3L-D, the drift of 4-story has decreased by 10.08%, which equals 1.16 cm. In WB1-H5-1.2L-T case, the 5-story drift decreased by 4.62%, by 1.24 cm, while in WB1-H5-1.4L-T case, the 5-story drift decreased by 26.15%.

As shown in Fig.12, for WB1-H10 model, the inter-story drift of the 5-story has been increased by 48.15%, which equals 1.2 cm in WB1-H10-1.4L-D case. In WB1-H10-1.2L-O case, the 7-story drift increased by 42.35%, or 1.21 cm. In WB1-H10-1.4L-T case, the 7-story drift increased by 36.47%, by 1.16 cm.

As shown in Fig.13, for WB1-H15 model, the inter-story drift of the 7-story has been increased by 27.42%, which equals 1.58 cm in WB1-H15-1.4L-D case. In WB1-H15-1.3L-O and WB1-H15-1.4L-O case, the 10-story drift increased by 6.06%, or 1.4 cm. In WB1-H15-1.3L-T case, the 12-story drift increased by 13.64%, by 1.5 cm.

7. NUMERICAL STUDY OF IRREGULAR DUAL SYSTEM WITH EFFECT OF INPLANE-DISCONTIUNITY IRREGULARITY.

7.1 Description of models and studied parameters

In the study of irregularities due to the discontinuity in lateral force resisting element, each set of floors includes a control structure with uniform stiffness across all floors. Additionally, three structures with in-plane discontinuity are

examined. The first structure has in-plane discontinuity irregularity applied to 1st, 2nd and 3rd level of H5, H10 and H15 sequentially. for the second group in-plane discontinuity irregularity applied to 2nd ,4th and 5th level of H5, H10 and H15 sequentially. The third position the in-plane discontinuity irregularity located at 3rd, 7th and 10th level of H5, H10 and H15 sequentially for the third group., as shown in Fig.14 and 15. The in-plane discontinuity characteristics vary by adjusting the location of the shear wall at each level to not be continuous to its base, introducing a comprehensive exploration of the impact of in-plane discontinuity irregularities on structural behavior. Table 10 summarize the studied structures with different irregularities conditions.

7.2 Results and discussion

These systems were run for nonlinear static pushover analysis using SAP 2000 [9]. The ductility reduction factor Rμ, overstrength factor Rs, and response factor R were deduced by equations 1, 2, 3, and 4 sequentially, and the results are listed in Table 11.

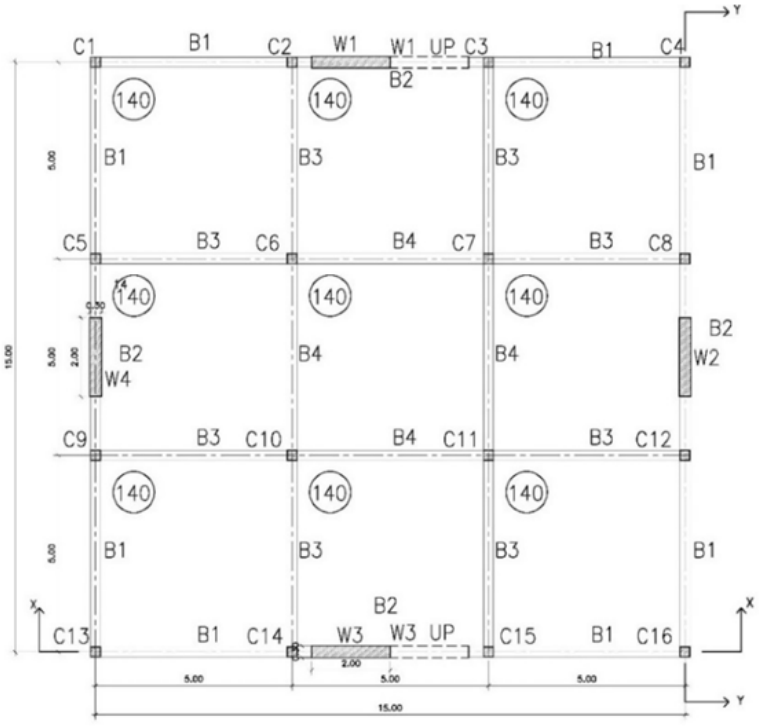

FIGURE 14. The structure plan of WB2.

TABLE 10. Configurations of the second system**.**

Specimen name	Number of stories	Type of irregularity	Severity of irregularity	Place of influence	Group
WB2-H5	5	------	------	------	WB2-H5
WB2-H5-D	5	In-plane discontinuity	____	First floor	
WB2-H5-O	5	In-plane discontinuity	____	Second floor	
WB2-H5-T	5	In-plane discontinuity	------	Third floor	
WB2-H10	10	____	____	____	WB2-H10
WB2-H10-D	10	In-plane discontinuity	____	Second floor	
WB2-H10-O	10	In-plane discontinuity	____	Fourth floor	
WB2-H10-T	10	In-plane discontinuity	____	Seventh floor	
WB2-H15	15	------	------	------	WB2-H15
WB2-H15-D	15	In-plane discontinuity	____	Third floor	
WB2-H15-O	15	In-plane discontinuity	____	Fifth floor	
WB2-H15-T	15	In-plane discontinuity	------	Tenth floor	

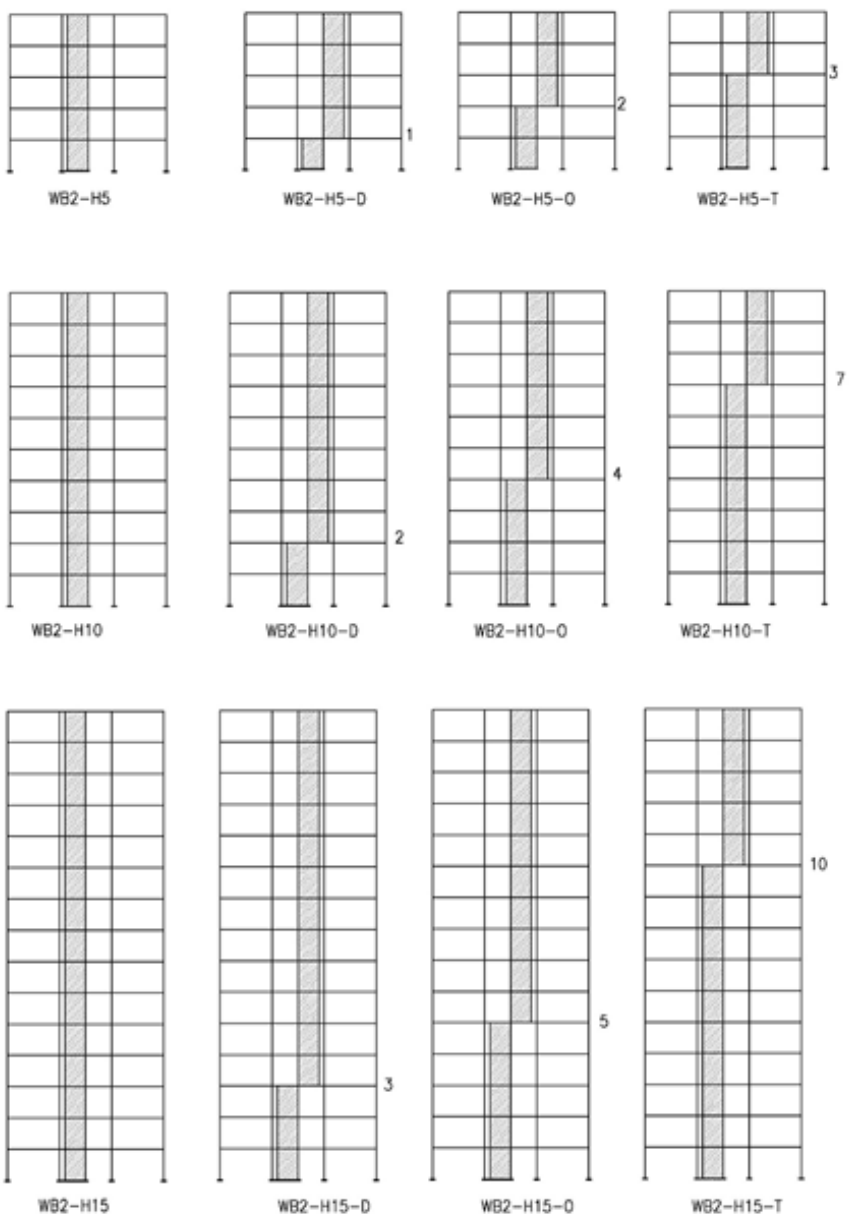

FIGURE 15. Dual system with effect of in-plane discontinuity irregularity.

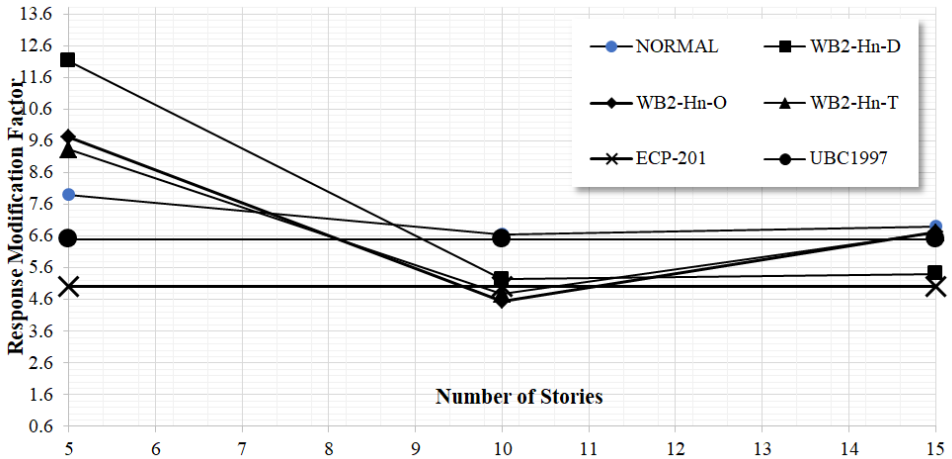

FIGURE 16. Response modification factors versus number of stories for the Second system models with in-plan discontinuity in down, one-third and two third floor to the normal case.

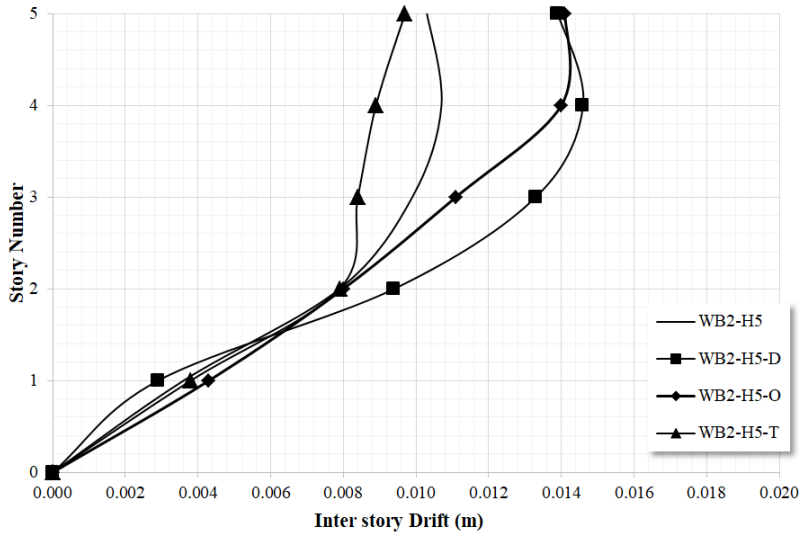

FIGURE 17. Story inter-drift profile for WB2-H5 in down, one third and two third case.

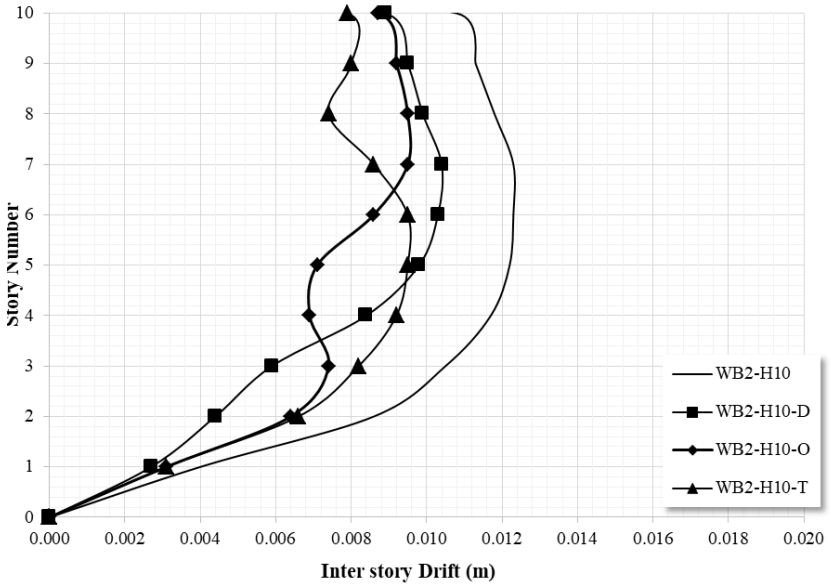

FIGURE 18. Story inter-drift profile for WB2-H10 in down, one third and two third case.

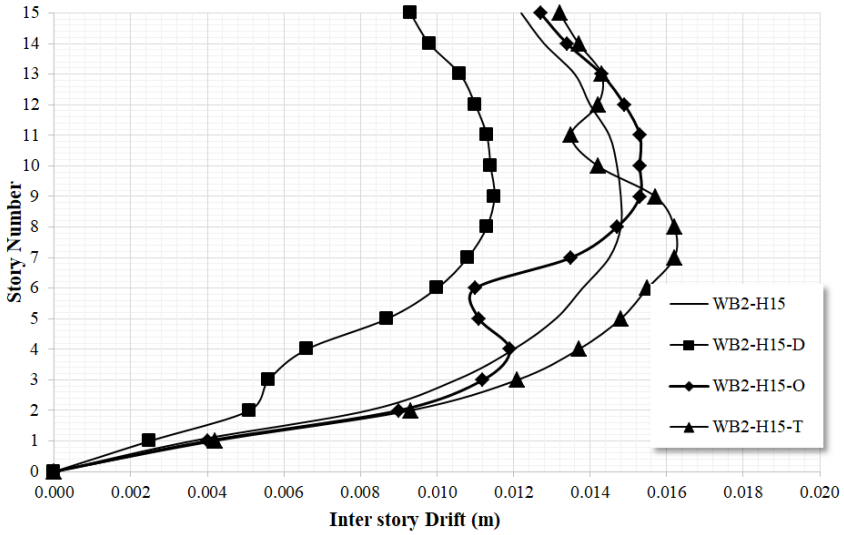

FIGURE 19. Story inter-drift profile for WB2-H15 in down, one third and two third case.

As shown in Table 11 according to the change in structure high, for WB2-H10 case, the response modification factor is decreased by 16%. Then, decreased by 13% for WB2-H15. According to the in-plan discontinuity distribution, for WB2-H10-T the R factor decreased by 28%, for WB2-H15-D there was a significant decrease in R value by 21% and for WB2-H15-.8K-O , for WB2-H5-D there was a significant increase in R value by 53% .

As shown in Table 11, in WB2-H5 model, the story displacement is highly affected by the discontinuity irregularity. While WB2-H5-D, the displacement of the fifth story increased by 27.59%, while the first or second story did not affect it remarkably. In the case WB2-H5-T, the displacement of the fifth story decreased by 8.73%, while the first story did not affect remarkably.

Second, for WB2-H10 model, the story displacement is highly affected by the discontinuity irregularity. As shown in Table 11, while WB2-H10-D and one WB2-H10-O, the displacement of the 10-story decreased by 24% and 27.58%. while the first story did not affect me remarkably. In the case WB2-H10-T, the displacement of the 10-story decreased by 26.07%.

Third, for WB2-H15 model, the story displacement is slightly affected by the discontinuity irregularity except for WB2-H15-D case. As shown in Table 11, while WB2-H15-D, the displacement of the 15-story decreased by 27.58%, while WB2-H15-O caused an increase in 15-story displacement by 0.27%.

As shown in Table 11 and Fig.17 for WB2-H5 model, the inter-story drift of the 3-story has been increased by 34.34%, which equals 1.39 cm at WB2-H5-D. In WB2-H5-T case, the 3-story drift decreased by 15.15%, or 0.97 cm.

Figure 18, for WB2-H10 model, the inter-story drift of the 3-story has been decreased by 43.81%, which equals 0.59 cm at WB2-H10-D. In WB2-H10-O, the 6-story drift decreased by 30.08%, by 0.86 cm. In WB2-H10-T case, the 9-story drift decreased by 29.20%, or 0.8 cm.

Figure 19, for WB2-H15 model, the inter-story drift of the 4-story has been decreased by 45%, which equals 0.66 cm at WB2-H15-D. In WB2-H15-O, the 13-story drift increased by 5.15%, or 1.43 cm. WB2-H15-T case, the 9-story drift increased by 6.08%.

8. CONCLUSION

- The values of the R coefficient listed in the design codes cannot be similar to any of those deduced from concrete structures designed by the Egyptian code or any of the other codes, as it is deduced based on two main coefficients: the ductility reduction factor and the overstrength factor. The study also proved that the values of the R-coefficient vary significantly from one structure to another in the event of a change in the number of stories and geometry.
- The value of the R coefficient in the case of dual systems, is inversely proportional, as it decreases by increasing the height by about 36%.
- The value of the ductility reduction factor is directly proportional to the number of stories. In the case of dual systems, the R coefficient is inversely proportional, as it decreases by increasing the height by about 17%.
- The coefficient R decreases by significant percentages if there are geometric irregularities in structures that are equal to or less than 5 floors, and the more the number of floors increases, the more the value of the coefficient increases to reach its peak in structures consisting of 10 floors, and then gradually begins to decrease the effect of the increase on the coefficient. In the case of 1.4L-T, we find that there was a decrease of 38% for structures with 5 floors and an increase of 38% in the structure with 10 floors, and the increase value decreased to up to 3% in a 15-story building. The maximum effect on the R coefficient occurs in case of a geometric irregularity in the upper part of the building.
- Regarding to the effect on R coefficient, the geometrical irregularity is inversely proportional to the impact of in-plane discontinuity. where the coefficient R increases by significant percentages if there are discontinuous irregularities in structures that are equal to or less than 5 floors, and the more the number of floors increases, the more the value of the coefficient decreases to reach its peak in structures consisting of 10 floors, and then gradually begins to increase the effect of the decrease on the coefficient. In the case WB2-H5-D model, the R increased by 53% while WB2-H10-D model decreased by 21%. The maximum effect on the R coefficient occurs in case of an in-plane discontinuity irregularity in the lower part of the building.
- The average R values that were deduced for structures consisting of 15 and 10 floors in the case of geometric, in-plane discontinuity, their value is 5.8, and in the case of structures consisting of 5 floors, 9.78.

REFERENCES

[1] Research Center for Housing and Building (2020), “Egyptian code for design and construction of reinforced concrete buildings (ECP-203)”, Giza, Egypt.

[2] Research Center for Housing and Building (2012), “Egyptian code for calculation of loads and forces for buildings (ECP-201)”, Giza, Egypt.

[3] Humar, J. L., and E. W. Wright (1977), “Earthquake response of steel-framed multistorey buildings with set-backs”, Earthquake Engineering & Structural Dynamics, 5(1), 15-39. https://doi.org/10.1002/eqe.4290050103.

[4] Aranda, G. R. (1984), “Ductility demands for R/C frames irregular in elevation”, Proceedings of the 8th World Conference on Earthquake Engineering, San Francisco, U.S.A., July.

[5] Bahrain M. Shahrooz and Jack P. Moehle (1990), “Seismic response and design of setback buildings”, Journal of Structural Engineering, 116(5). https://doi.org/10.1061/(ASCE)0733-9445(1990)116:5(1423)

[6] Sharon L. Wood (1992), “Seismic response of R/C frames with irregular profiles”, Journal of Structural Engineering, 118(2). https://doi.org/10.1061/(ASCE)0733-9445(1992)118:2(545)

[7] Ruiz S. E., E. Rosenblueth, and R. Diederich (1989), “The Mexico earthquake of September 19, 1985—Seismic response of asymmetrically yielding structures”, SAGE Journals. https://doi.org/10.1193/1.1585513

[8] Mwafy, Aman, and Sayed Khalifa (2017), “Effect of vertical structural irregularity on seismic design of tall buildings”, The

Structural Design of Tall and Special Buildings, 26(18), e1399. https://doi.org/10.1002/tal.1399

[9] CSI (2020), "SAP2000 v18.2.0 is an intermediate update from SAP2000 v18.0.0 through v18.1.1", available from https://csiamerica.com.

[10] International Conference of Building Officials (1997), "Uniform building code", ISBN 1884590942, 9781884590948.

[11] Miranda, Eduardo, and Vitelmo V. Bertero (1994), "Evaluation of strength reduction factors for earthquake-resistant design", Earthquake Spectra, 10(2), 357-379. https://doi.org/10.1193/1.1585778

[12] American Society of Civil Engineers (ASCE)/SEI (2016), "Minimum design loads for buildings and other structures", Virginia, U.S.A.

[13] Cansiz, S. (2023), "Analytical investigation of the measures to be taken against weak storey irregularities", Revista de la Construcción. Journal of Construction, 22(2), 407-418. https://doi.org/10.7764/RDLC.22.2.407.

[14] Seismosoft (2022), "SeismoBuild 2022 – A computer program for seismic assessment and retrofitting of RC structures", available from https://seismosoft.com/.

[15] Bhatt, Vandit (2019), "Pushover analysis of RCC set back building using SAP2000", International Journal for Research in Applied Science & Engineering Technology (IJRASET), 7(XI), Nov 2019, available at www.ijraset.com.

[16] IS (1987), "Code of practice for design loads (other than earthquake) for buildings and structures, Part 2: Imposed loads", [CED 37: Structural Safety].

[17] Tarsha, Ihssan, and Shadi Fattoum (2016), "Usage of nonlinear static analysis for dual systems", AL-Baath university journal, 38.